

Upcycling Waste Polypropylene with Basalt Fibre Reinforcement Enhancing Additive Manufacturing Feedstock for Advanced Mechanical Performance

Pouyan Ghabezi^{1, 2, 3*}, Omid Sam-Daliri^{1*}, Tomas Flanagan⁴, Michael Walls⁵, Noel M. Harrison^{1, 2, 3}

¹ College of Science and Engineering, University of Galway, Galway, Ireland;

² I-Form, the SFI Research Centre for Advanced Manufacturing, Ireland

³ Ryan Institute for Environmental, Marine and Energy Research, University of Galway, Galway, Ireland

⁴ Éire Composites Teo, Údarás Industrial Estate, An Choill Rua, Inverin, Co., Galway, Ireland;

⁵ CTL Tástáil Teo, Údarás Industrial Estate, An Choill Rua, Inverin, Co., Galway, Ireland;

* Correspondence: pouyan.ghabezi@universityofgalway.ie, omid.samdaliri@universityofgalway.ie

Abstract

This research seeks to overcome the printing and processing challenges of using waste polypropylene (PP) reinforced with short basalt fibres, transforming them into upcycled feedstock for additive manufacturing. It introduces an optimised method for producing filaments and 3D printing with these materials, addressing common issues such as adhesion and warpage through innovative techniques while achieving maximum mechanical performance in the resulting composites. Basalt fibre weight fractions of 0%, 2%, 5%, 8%, 15%, 30%, and 50% were used to reinforce the recycled polypropylene, improving both printability and mechanical properties. The tensile strength reached 53.58MPa at 15% fibre content, while the flexural strength peaked at 34.06MPa with 30% fibre content, revealing distinct interactions between the fibres and polymer under tensile and flexural loading that were not previously observed. Microstructure, voids, debonding, and dispersion were examined using optical and scanning electron microscopy. Differential Scanning Calorimetry (DSC) was performed to assess the thermal behaviour and crystallinity of the recycled polymer during filament production and printing, revealing slight matrix degradation during these processes. The findings highlight the potential of waste basalt fibre-reinforced PP as a valuable filament feedstock for 3D printing, supporting a circular economy approach to composite manufacturing.

Keywords: 3D printing, Recycling, Basalt fibre, Circular economy, polypropylene

1. Introduction

The use of composites is on the rise, with the global market projected to reach USD 131.6 billion by 2024 (up from USD 90.6 billion in 2019). However, this growth also leads to a significant amount of waste generated from manufacturing processes, including post-industrial trimmings and off-cuts of composite materials [1, 2]. Although composites are favoured for structural marine, civil, or sporting industries, waste generation during their production remains a major challenge.

The use of recycled thermoplastics in material extrusion additive manufacturing (MEX one of the more popular forms of 3D printing, often reported as common tradenames Fused Deposition Modelling (FDM), or Fused Filament Fabrication (FFF)) has gained attention in recent years due to environmental concerns and the desire to reduce waste. Typical MEX 3D printing, using a 1.75mm thermoplastic filament, melts the material in a print head, selectively dispensing it through a nozzle in a layer by layer format on a build plate, creating three-dimensional objects from digital designs [3]. Short fibre reinforcements can also improve the mechanical properties of recycled thermoplastic composites [4-6]. However, there are several challenges associated with filament making and 3D printing of recycled thermoplastics in the presence of short fibres. The first challenge is the quality of the recycled thermoplastic material used for filament making. Recycled materials often contain impurities and contaminants that can affect the properties of the final product. The presence of short fibres can also make the material more difficult to process during filament making due to agglomeration and poor dispersion [7]. The orientation and alignment of the short fibres during the filament making process and MEX printing can also affect the mechanical properties of the composite. Achieving a uniform and consistent orientation of the fibres can be challenging, especially for complex geometries and intricate designs [8, 9]. The presence of chopped fibres in the melt increases its viscosity and introduces heterogeneity in the coefficient of thermal expansion[10]. Another challenge is achieving a consistent uniform circular cross-section of the filament. This is essential for trouble-free feeding and extrusion during MEX [11]. Inconsistent filament diameter can lead to clogging, under-extrusion, and uneven printing quality [12]. The extrusion temperature must also be carefully controlled during filament making. Too high of a temperature can cause degradation of the recycled material, while too low of a temperature can result in poor adhesion between the short fibres and the matrix material [13]. Also, poor adhesion can result in delamination, voids, and other defects, which can significantly reduce the mechanical properties of the final 3D printed product [14]. Another challenge is the optimisation of printing parameters such as layer thickness, printing speed, and infill density. These parameters can affect the interfacial properties of the composite, including adhesion strength and interlayer bonding. Optimisation requires a thorough understanding of the material properties and the printing process [15-18]. The presence of fibres can also affect the surface finish and visual appearance of the printed part. Poor fibre dispersion can result in a rough surface finish and visible defects, which can be undesirable for some applications [19, 20].

Almeshari et al. [21] developed a MEX filament made of short carbon fibre (SCF) reinforced polypropylene (PP) composite with varying SCF content. The resulting composites showed improved tensile strength and impact toughness, with the 22% SCF/PP composite having the highest improvement. However, strain at break values decreased up to 11 wt.% SCF content and then dropped suddenly in the composite with 14 wt.% SCF. Off-cuts of basalt fibre and recycled polypropylene mushroom trays were combined in an

extruder to produce short-fibre-reinforced filaments for 3D printing [22]. Filaments with low basalt fibre weight fractions (max. 8%) were produced and optimised for quality using the Noztek Touch Dual PID filament maker. Microscopic and differential scanning calorimetry assessments were carried out, and the tensile strength and elastic modulus of the reinforced recycled polypropylene were measured. Cai et al. [23] investigated the effect of printing parameters on the interfacial properties of 3D-printed natural continuous ramie fibre reinforced polypropylene composites. The interlayer and intralayer interfacial properties were studied and machine learning methods were used to optimise the printing parameters for improved interfacial performance. Bending tests were conducted, confirmed that specimens with weak interfacial strength had poor mechanical properties, with interlaminar delamination failure under bending loads. Nylon polymer reinforced with glass and carbon fibre with different raster orientations (0° , 45° , 90°) were 3D printed and evaluated for mechanical properties [24]. Nylon reinforced with glass fibre showed high stiffness (higher resist bending forces), while nylon with carbon fibre exhibited elastic behaviour, lower flexural strength, and higher deflection. Effective stress transfer at the fibre/matrix interface improved flexural strength. Dynamic mechanical analysis and scanning electron microscopy (SEM) analyses confirmed enhanced interfacial interaction. The research provides valuable insights into the structural behaviour and mechanical properties of 3D printed nylon composites, applicable in various end-uses [24]. Vetrnam et al. [25] reported on the 3D printing and mechanical characterization of high specific strength, high-temperature Polyamide 6 (Onyx), continuous glass-fiber reinforced Onyx, and carbon-fiber reinforced Onyx composites. The Onyx + CF composites exhibited significant improvements in mechanical properties, with elastic modulus and tensile strength increasing by up to 1243% and 1344%, respectively, compared to neat Onyx samples. Yang, et al. [26] investigated the flow of short fibre reinforced thermoplastic composites during MEX. Visual and quantitative analysis revealed variations in fibre orientation, length, and fraction, as well as void formation. Nozzle geometry affects fibre alignment, while fibre length decreases due to collisions with the nozzle wall. Voids primarily occur during extrusion and decrease in on-bed printing. The experimental data can serve as benchmarks for computational models of MEX of short fibre reinforced composites. Sang et al. [27] developed KH550-treated basalt fibre (KBF) reinforced PLA composite filaments. PLA/KBF shows comparable tensile properties to neat PLA, superior flexural properties, and confirmed feasibility for 3D printing, offering a cost-effective option for complex designs. Nectarios et al. [28-30] demonstrated the potential of using recycled Glycol-modified polyethylene terephthalate (PETG), Polypropylene (PP), Thermoplastic Polyurethane (TPU) and acrylonitrile-butadiene-styrene (ABS) in consecutive 3D printing cycles. Mechanical and thermal responses were tested using Distributed Recycling Additive Manufacturing (DRAM) equipment over six recycling cycles. The results showed only minor effects on the mechanical and thermal properties of PETG after six recycling rounds.

MEX 3D printing technology commonly employs thermoplastic materials such as polylactic acid (PLA), polyamide (PA), acrylonitrile butadiene styrene (ABS), polycarbonate (PC), Polyether ether ketone (PEEK) [31-33]. However, there is a gap in research concerning filament production and 3D printing using recycled thermoplastics. Typically, MEX-printed thermoplastic parts are not suitable for load-bearing applications, making them primarily useful for prototyping or non-load bearing components. However, researchers have conducted numerous studies aiming to enhance the strength of filament fabricated through MEX 3D printing, thereby addressing this limitation. The concept of using domestic polypropylene waste (e.g. vegetable packaging) as a supplementary source of raw thermoplastic material to adjust the fibre volume fraction for the composite material has also been demonstrated [24, 34]. The incorporation of basalt fibres into the polypropylene matrix has the potential to enhance the mechanical properties of the composite material, making it suitable for various applications, including automotive, construction, and aerospace industries.

This study introduces a novel approach that incorporates waste off-cut short basalt fibres, sourced from composite industries, into upcycled polypropylene materials, specifically recycled mushroom containers. The goal was to address the printing challenges associated with polypropylene waste, such as adhesion and warpage issues, while enhancing the mechanical strength and printability of the materials through the addition of short fibres, which alter the dynamic flow during both filament production and 3D printing. To achieve this, the research focused on optimising the material extrusion process and 3D printing parameters, including temperature, speed, and adhesion strategies, to produce standard test specimens. A comprehensive evaluation was conducted, involving mechanical tests (tensile and flexural) and microscopic analyses (Optical Microscopy and SEM), to assess the impact of short basalt fibre incorporation on the quality of filament production and material extrusion (MEX) 3D printing.

2. Materials

Basalt fibre offers superior strength and stiffness compared to E-glass, along with environmental safety, non-toxicity, corrosion resistance, and non-magnetism. Additionally, it boasts high thermal stability and excellent insulation properties [35]. Polypropylene trays commonly used for domestic mushroom cultivation were gathered and subjected to sorting, washing, and shredding into small flakes not exceeding 5 mm in length. In this study, off-cuts of Mafic basalt fibres were chosen as the reinforcement material due to their high strength, durability, and resistance to chemical and thermal degradation. The waste basalt fibres were collected from EireComposites Teo, a composite manufacturing company in Ireland. The short fibres had an average length of 3mm and an average diameter of 16 μm . The mechanical properties of the short basalt fibres used in this study were as follows [36]: Tensile Strength (ASTM D2343) = 3100 MPa, Tensile

Modulus (ASTM D2343) = 88-92 MPa, Elongation at Break = 3.5%, and Density according to DIN 65569 = 2.63 g/cm³.

3. Material Extrusion and 3D Printing

The quality of filament in 3D printing is critical for achieving accurate and consistent prints. In this study, the filaments were produced using a **Noztek Touch Dual PID filament maker** with short basalt fibre weight fractions of 0%, 2%, 5%, 8%, 15%, 30%, and 50% into Polypropylene thermoplastic (Figure 1). The optimised filament making process are summarized in Table 1. The temperatures at the nozzle tip and barrel were adjusted based on the weight fraction.

For basalt fibre weight fractions of 0%, 2%, 5%, and 8%, the temperatures at the nozzle tip and barrel were 220°C and 225°C, respectively. The RPM was set to 12, and the cooling fan was turned off. While for basalt fibre weight fractions of 15%, 30%, and 50%, the temperatures at the nozzle tip and barrel were recorded as 230°C and 235°C, respectively.

Table 1: Optimised filament making parameters.

Code	Basalt Fibre Wt.	T1	T2	Diameter
PP	0%	220°C	225°C	1.55mm
PP+2%BF	2%	220°C	225°C	1.55mm
PP+5%BF	5%	220°C	225°C	1.50mm
PP+8%BF	8%	220°C	225°C	1.50mm
PP+15%BF	15%	225°C	230°C	1.45mm
PP+30%BF	30%	225°C	230°C	1.35mm
PP+50%BF	50%	225°C	230°C	1.35mm
Conditions: RPM = 12, Fan: Off				
T1= Nozzle Tip Temperature, and T2= Barrel Temperature				

To make the filament reinforced with different fibre weight fractions, the mix of fibre and thermoplastic was double extruded as shown in Figure 1 to reach the highest fibre/matrix adhesion and impregnation a long with desired fibre distribution. The average length of short basalt fibres was measured as 1.3mm after double extrusion for the reinforced filaments. It is worth noting that the materials with high fibre weight fractions and higher fibre length (than what was recommended above) are not printable (or hard to print) and have low quality (high viscosity, nozzle clogging, high void content and unfilled regions, etc.).

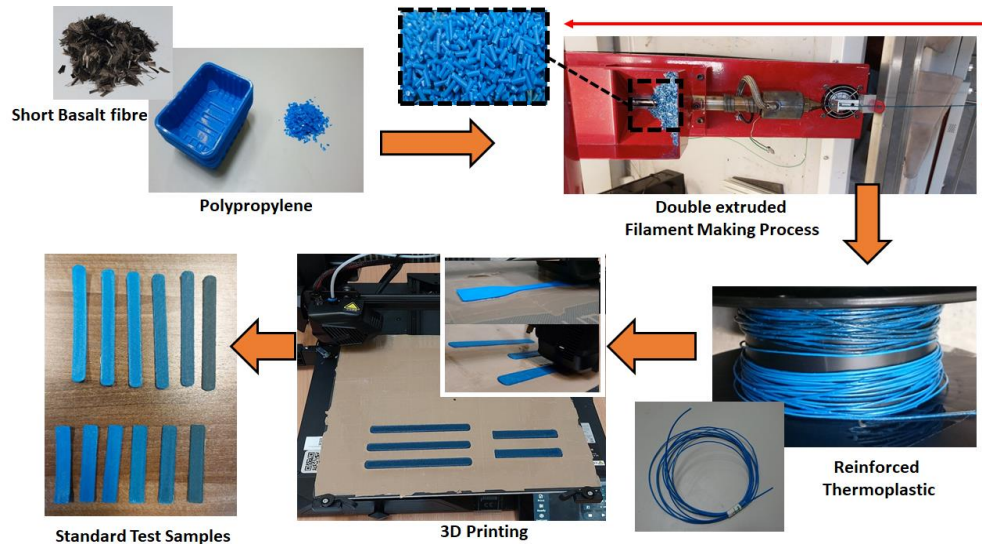


Figure 1: Filament making and 3D printing of recycled polypropylene and short basalt fibre.

The filaments produced were subjected to quality control measures including diameter size and surface finish. The diameter of the filament was measured using a digital calliper, and the average diameter was calculated. The surface finish of the filament was visually assessed for smoothness and any signs of inconsistencies (change in diameter, waviness, ovality, etc.). Producing the filament with a constant diameter in presence of short fibre is difficult. The optimised parameters in Table 1 were used to reach the best quality in terms of diameter consistency. Overall, there is a trend of decreasing filament diameter as the weight fraction of basalt fibre increases, indicating that the presence of basalt fibre affects flow dynamics (reduces the die swell) and the consolidation of the composite filaments.

A Creality Smart-10 3D printer with a nozzle diameter of 0.8mm was used to print the reinforced filaments with short basalt fibre. Achieving proper adhesion between the printed object and the bed surface is a significant hurdle in MEX 3D printing of polypropylene (PP) materials. A range of approaches (Figure 2) were explored to minimise the peeling of the thermoplastic from the build plate. Rafts are typically used to provide a larger surface area for better adhesion, but in this case, it did not work as expected because the raft material was the same material as the object was and polypropylene did stick to the built plate. Similarly, the use of a brim, which is a thin extension around the base of the object, did not provide sufficient adhesion. These methods might have failed due to issues such as insufficient contact area or inadequate bonding between the raft/brim and the bed surface. The application of glue (manufactured for PP filaments) also did not prove to be effective for the recycled PP. Glue is commonly used to improve adhesion, but for this material, it did not provide the desired results.

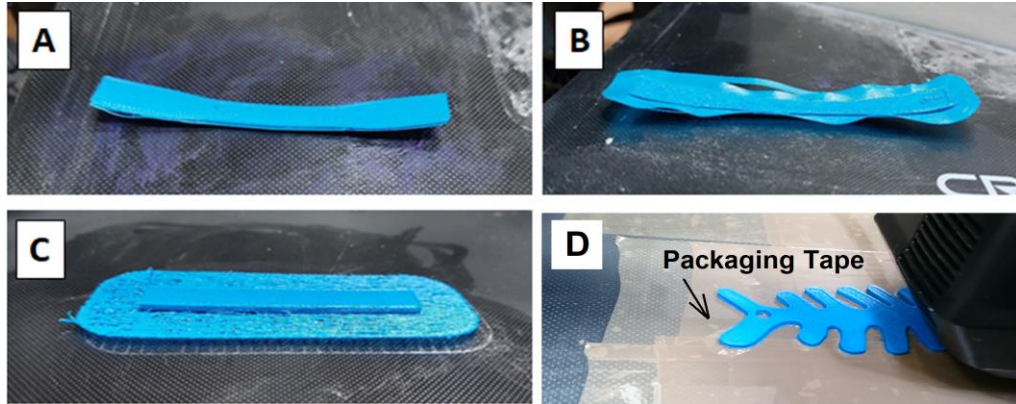


Figure 2: Different strategies to improve the adhesion to the built plate. A) Glue, B) Brim, C) Raft, D) 3 layers of PP packing tape.

After examine different adhesion techniques, use of three to four layers of polypropylene (PP) packing tape on the bed with optimised effective parameters was successful in achieving desirable adhesion (Figure 2- D and E). Widely available PP packing tape can provide a smooth and adhesive surface for the object to adhere to the built plate during printing (the packing tape is stuck to the built plate and the PP built object securely attaches to the non-adhesive side of the packing tape made from the same material). Two to three layers of tape created an optimum surface for adhesion, ensuring that the printed object firmly adhered to the bed. The parameters mentioned below are crucial for optimising the MEX process specifically for printing PP (Polypropylene) reinforced with short basalt fibres. The optimised settings provide a balance between print quality, dimensional accuracy, adhesion, and print speed, taking into account the unique characteristics and requirements of PP reinforced with short basalt fibres. However, it is important to note that these parameters may still require fine-tuning based on specific printer models, filament properties, and desired outcomes.

The optimisation of 3D printing parameters began by exploring the ideal printing temperatures for extruding PP materials reinforced with different weight fractions of short carbon fibres. This involved experimentation with nozzle sizes (from 0.4mm to 0.8mm) and temperature settings (from 220°C to 270°C) to achieve optimal extrusion consistency and material flow. Subsequently, efforts were focused on mitigating challenges related to warpage and shrinkage, necessitating a thorough investigation into the optimal bed temperature (from room temperature to 60°C), layer height (from 0.1mm to 0.5mm), and effective adhesion techniques. This phase involved iterative testing to identify parameters that minimize warping and ensure strong adhesion between printed layers. Furthermore, analyses of flow rates (from 100% to 160%) and overlaps between walls and infill patterns, which are more critical with higher fibre weight fractions, were conducted to ensure the integrity of each printed layer and bead. These analyses, supported by microscopic imaging, provided details for optimising infill patterns to minimize interlaminar and

interbead voids and gaps. This resulted in enhanced print quality and structural integrity of the final printed components.

The optimised parameters for 3D printing PP (Print direction: $\pm 45^\circ$) reinforced with short basalt fibres are as follows (Table 2):

Nozzle Temperature: The optimal printing temperatures vary depending on the composition of the polypropylene (PP) filament. For non-reinforced PP and those with 2% wt. and 5% wt. Basalt fibre, a temperature of 245°C is recommended. PP reinforced with 8% BF is printed at 250°C, while PP with 15%, 30%, and 50% BF requires temperatures of 255°C. These temperatures are crucial to ensure proper melting and extrusion of the filament, especially in the presence of fibres that may influence flow dynamics.

Table 2: Optimised 3D printing process parameters.

Material	PP	PP+ 2% BF	PP+ 5% BF	PP+ 8% BF	PP+ 15% BF	PP+ 30% BF	PP+ 50% BF
Nozzle Temp. - °C	245	245	245	250	255	255	255
Bed Temp. - °C	45	45	45	45	45	45	45
1 st Layer Height-mm	0.2	0.2	0.2	0.2	0.25	0.25	0.25
Subsequent Layers Height - mm	0.25	0.35	0.4	0.45	0.45	0.45	0.45
Print speed mm/Sec	15	15	10	10	10	8	8
1 st Layer Flow Rate %	100	100	140	140	140	140	140
Subsequent Layers Flow Rate %	120	120	160	160	160	160	160

Bed temperature and adhesion: The bed temperature remained consistent at 45°C across all compositions. While less critical than other printing parameters, it ensures sufficient adhesion, particularly for fibre-reinforced specimens known for their reduced warping tendency. Adhesion was further enhanced using 3-4 layers of PP packing tape, as polypropylene does not naturally adhere to the built plate. Instead, the one-side adhesive packing tape sticks to the bed, while the printed materials adhere to the other side (Figure 2- D).

Layer Height: The choice of first layer height varied based on the fibre weight fraction, ranging from 0.2mm to 0.25mm for lower fractions and 0.25mm for higher fractions. Subsequent layers were adjusted to 0.25mm for PP, 0.35mm for PP+2%CF, 0.4mm for PP+5%CF, and 0.45mm for the other specimens. This optimisation strategy ensures proper adhesion to the build surface with thinner initial layers while preventing nozzle clogging and maintaining print quality and speed with thicker subsequent layers.

Print Speed: The recommended print speeds also vary depending on the composition: 15mm/s for PP and PP+2% BF, 10mm/s for PP+5% BF, PP+8% BF, PP+15% BF, and

8mm/s for PP+30% BF and PP+50% BF. Optimising print speed is crucial as it impacts printing time and quality. Lower speeds are advisable for higher fibre percentages to ensure proper adhesion between infill beads and printed walls.

Flow Rate: The flow rate for the first layer was 100% for PP and PP+2% BF, and 140% for the other samples. Subsequent layers had a flow rate of 120% for PP and PP+2% BF, and 160% for the other fibre-reinforced samples. This adjustment ensures proper extrusion and prevents unfilled regions near walls, crucial for maintaining print quality and structural integrity.

Printing with materials with both high fibre weight fractions and longer fibre lengths can lead to significant challenges in 3D printing. A high fibre content or longer fibres can lead to agglomeration within the printing material. This can disrupt the uniform flow of the material and cause nozzle clogs or irregular extrusion, negatively impacting the print quality. High fibre content and longer fibres can block the material's flow through the printer nozzle, making it difficult for the printer to deposit and adhere layers properly.

Adding a high content of short fibres, such as 50 wt.% basalt or other reinforcing fibres, to polymers like polypropylene (PP) significantly alters their processability. Short fibres enhance the mechanical properties of the polymer, such as tensile strength, stiffness, and thermal stability, but they also introduce several challenges during both filament production and 3D printing. These challenges primarily come from the increased viscosity of the composite material and the non-uniform flow characteristics introduced by the dispersed fibres. To address these difficulties, double extrusion is a commonly employed technique for producing printable filaments. The first extrusion step helps blend the fibres uniformly within the polymer matrix, ensuring consistent distribution. Without adequate dispersion, fibres tend to agglomerate, which can lead to uneven mechanical properties and compromised part quality. The second extrusion refines the filament further, promoting better fibre alignment along the extrusion direction, which is crucial for improving the filament's mechanical performance and printability. By performing double extrusion, the risk of nozzle clogging or print defects caused by poorly distributed fibres is reduced. Even with double extrusion, printing fibre-reinforced polymers like PP+50 wt.% requires special adjustments to the printing process. The addition of short fibres increases the composite's viscosity, making it more resistant to flow. To overcome this, a higher extrusion temperature is employed, which lowers the melt viscosity and allows for smoother flow through the printer nozzle. However, the increase in temperature must be carefully controlled to avoid degradation of the polymer matrix, which could adversely affect the final properties of the printed part. Another important adjustment is the use of a higher layer height during the printing process. A higher layer height allows more material to be deposited per layer, compensating for the reduced flowability of the fibre-reinforced composite. This helps in achieving better interlayer adhesion and reduces the chances of

layer delamination or incomplete bonding between printed layers, which are common issues when printing high-fibre-content composites

4. Testing

A ZwickRoell Uniaxial tensile machine with a 1 kN Load cell was employed to test the short basalt fibre/PP filaments. The test speed of 2mm/min was selected based on previous studies and the author's experience for tensile testing of the filaments [5]. The filament gauge length of 70mm was chosen as it provides an appropriate length for capturing the deformation behaviour of the filaments (five test samples per composition).

In this study, the elastic properties of 3D printed polypropylene (PP) component specimens reinforced with short basalt fibre were also investigated through uniaxial tensile testing. The tests were conducted using an Instron 4467 machine equipped with a 30kN load cell at a crosshead displacement rate of 2mm/min, in accordance with ASTM D3039 (Five test samples per composition). The dimensions of the specimens were 120mm in length, 12mm in width, and 2mm in thickness. For comparison with the tensile strength of reinforced filaments, pure PP specimens in a dog-bone shape were tested based on ASTM D638 (Five test samples). Furthermore, the flexural strength of different 3D printed PP specimens was determined in accordance with ASTM D7254 (Five test samples per composition), using the same Instron 4467 machine with a crosshead speed of 1mm/min. The specimens had dimensions of 77mm in length, 13.3mm in width, and 2mm in thickness. Overall, these tests allowed for a comprehensive characterization of the elastic and flexural properties of 3D-printed PP specimens reinforced with short basalt fibre. By comparing the results to those of pure PP specimens, the effects of the reinforcement on the mechanical behaviour of the material could be quantified and analysed.

Microscopy images were captured by an Olympus BX51M microscope with a UC30 camera and were then analysed using image processing techniques to assess the fibre volume fraction, filament quality, and 3D printing quality (both surface texture and cross section) of the produced specimens. Scanning electron microscopy was employed via a Hitachi S-4700 FE-SEM (Resolution: 1.5nm) to characterize the fracture modes observed in both the filaments and the 3D printed specimens.

To analyze the thermal characteristics of recycled PP, Differential Scanning Calorimetry (DSC) was performed using a DSC 214 Polyma system with Proteus® 7.0 software from NETZSCH. Samples, weighing less than 10mg, underwent temperature scans from 40°C to 250°C at a heating rate of 20°C/min under an air flow of 50mL/min. Each group (raw material, filament, and 3D printed material) comprised five samples. Scans involved heating from 40°C to 250°C, cooling from 250°C to 40°C, and reheating and cooling again. Samples were held at 40°C and 250°C for 5 minutes during all scans to ensure thermal equilibrium.

5. Results and Discussion

5.1. Tensile Testing of Filament

The results in Table 3 provide insights into the impact of adding varying percentages of short basalt fibres to PP filaments in terms of tensile strength (a measure for quality control). From the data, it is observed that generally the tensile strength of the PP filament increased as the percentage of basalt fibres (BF) increased. This trend is evident from the baseline PP filament (31.79MPa) to the higher percentages of basalt reinforcement, such as PP-15%BF (53.58MPa) and PP-30%BF (49.66MPa). The highest tensile strength observed among the experimental results is 53.58 MPa for the PP-15%BF filament. It is worth noting that the tensile strength does not continuously increase with higher percentages of basalt reinforcement. These findings are significant for enhancing the mechanical properties of PP filaments, aiding in material selection and optimisation in various applications. The addition of fibres with high weight fractions can lead to processing challenges such as fibre agglomeration, weak interfacial bonding, improper fibre orientation, and void formation. These factors can ultimately result in a decrease in the tensile strength of the fibre-reinforced filaments and are further investigated using optical microscopy and SEM.

Table 3: Tensile test results for the filaments.

Materials	Tensile Strength - MPa
PP	31.79±2.66
PP -2% BF	35.49±1.71
PP -5% BF	38.19±2.37
PP -8% BF	40.60±1.18
PP -15% BF	53.58±2.31
PP -30% BF	49.66±1.22
PP -50% BF	35.36±1.11

5.2. Tensile Testing of 3D Printed Samples

The experimental results for 3D printed tensile tests of polypropylene (PP) reinforced with different percentages of short basalt fibre reveal a clear trend of increasing tensile strength with increasing fibre content up to a certain point, followed by a decrease in tensile strength beyond that point (Figure 3, Figure 4). The results indicated that the tensile strength of pure PP is 23.30MPa, which increases to 28.89MPa with the addition of 2% basalt fibres. The addition of basalt fibres at higher percentages resulted in a gradual increase in tensile strength up to 15% (36.36MPa) and a subsequent decrease in tensile strength at 30% (27.43MPa) and 50% (15.12MPa) basalt fibre content. The results shown in Figure 3 indicate that as the basalt fibre content increases, the strain in the PP composites decreases. This is expected as basalt fibres enhance the stiffness and rigidity of the composite, reducing its capacity to deform. However, there is a diminishing return beyond certain fibre content. For instance, the strain reduction becomes less pronounced when moving from

15% to 30% and 50% BF. This trend suggests that while higher fibre content improves stiffness, it also makes the material increasingly brittle and less capable of absorbing deformation. The substantial decrease in strain with higher fibre content underscores the effectiveness of basalt fibres in reinforcing the polymer matrix but also highlights a trade-off between stiffness and flexibility.

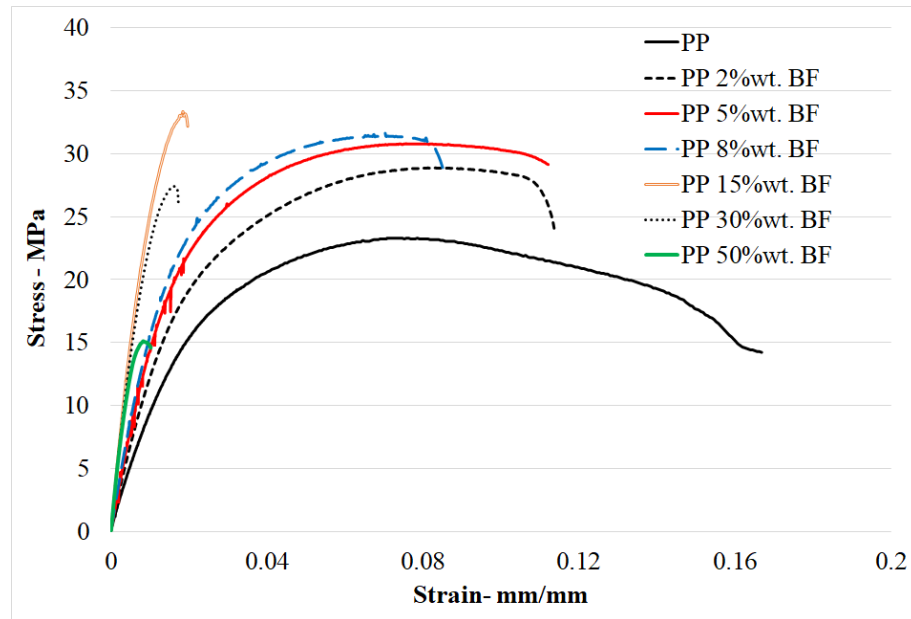


Figure 3: Stress-Strain diagrams for the tensile testing of of the 3D printed specimens.

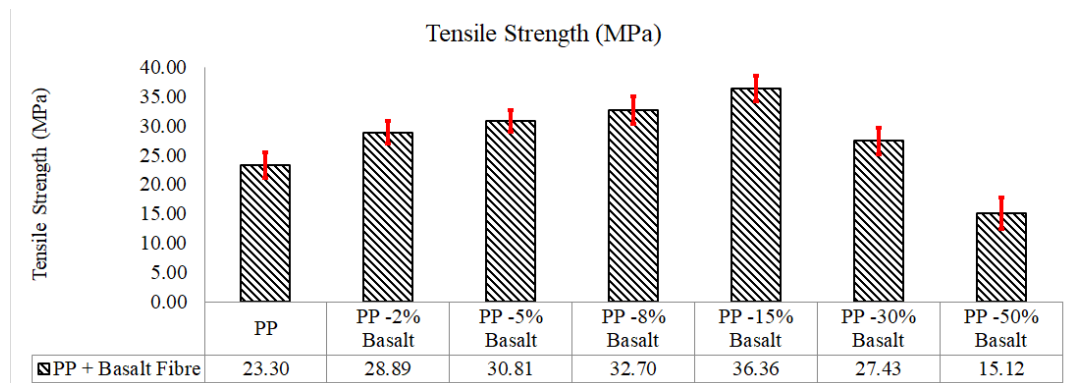


Figure 4: Tensile strength of 3D printed specimens (ASTM D3039)

The increase in tensile strength of PP with the addition of basalt fibres is due to the fibres' reinforcing effect on the polymer matrix. Basalt fibres are known for their high strength and stiffness, making them an ideal material for reinforcing polymer composites. The fibres form a network of reinforcement within the polymer matrix, enhancing its mechanical properties, particularly its tensile strength. As the percentage of fibres increases, the reinforcing network becomes denser, resulting in an increase in tensile strength. However, a further increase in basalt fibre content beyond 15% did not result in any improvement in

tensile strength. On the contrary, a decrease in tensile strength was observed at higher fibre contents. This decrease in tensile strength at higher fibre contents can be attributed to the formation of agglomerates or clusters of fibres, and void formation which can act as stress concentrators and promote premature failure of the composite material (this is discussed in the microscopy section). These clusters form due to the inability of the polymer matrix to uniformly distribute the fibres at higher concentrations, leading to stress concentrations that ultimately cause failure. The filaments with high fibre weight fractions were extrudable during the filament making process by a nozzle with 1.65mm (it is less than common 1.75mm due to the reduced die swell phenomenon), while printing these filaments have some challenges and produces defects in the printed specimens as it will be discussed in the microscopy section, the poor quality in the printed corners (in those with high fibre content) and debonding between the layers results in poor mechanical performance.

5.3.Three-Point Bending Testing

The experimental results of the three-point bending test on 3D printed polypropylene (PP) reinforced with different percentages of short basalt fibres indicated a clear trend of increasing flexural strength with the addition of basalt fibres up to a certain point (30% wt. basalt fibre), followed by a decrease in flexural strength beyond that point (Figure 5 and Figure 6). The results showed that the flexural strength of pure PP was 23.82MPa, which increased to 24.84MPa with the addition of 2% basalt fibres. The flexural strength increases gradually with the increase in basalt fibre content, reaching a maximum of 34.06MPa at 30% basalt fibre content (+43%). However, a further large increase in basalt fibre content beyond 30% led to a decrease in flexural strength (at 50% basalt fibre content). This decrease in flexural strength is due to the formation of fibre clusters or agglomerates, and also interbead voids (discussed in the microscopy section) which act as stress concentrators and promote premature failure of the 3D printed material.

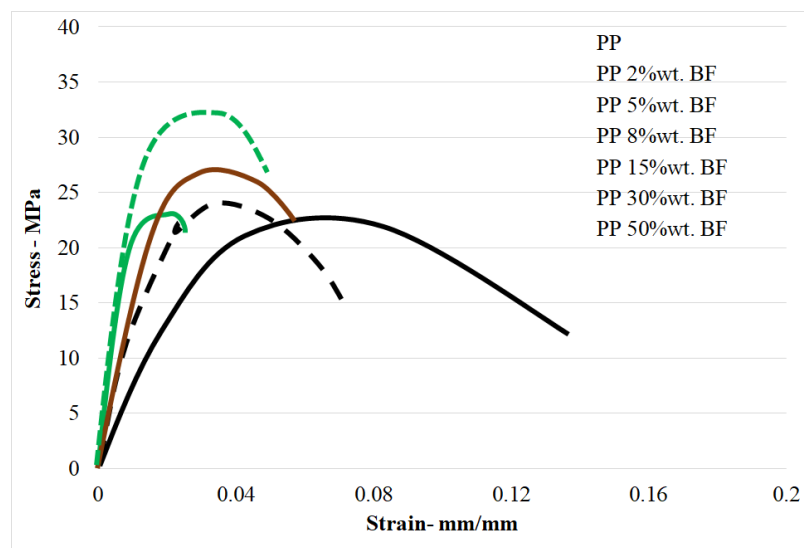


Figure 5: Stress-Strain diagrams for the tensile testing of of the 3D printed specimens.

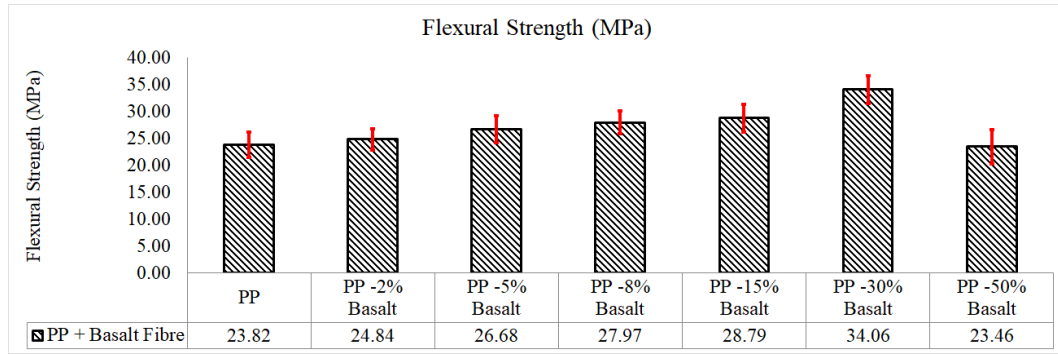


Figure 6: Flexural strength of 3D printed specimens (ASTM D7254)

5.4. Overall Discussion

The experimental results for tensile testing and flexural testing of 3D printed PP reinforced with different percentages of short basalt fibres show different trends and maximum values. The tensile testing results for the printed test samples show that the addition of basalt fibres leads to an increase in tensile strength up to 15% fibre content, beyond which the tensile strength decreases (The same was observed in testing of filaments). In contrast, the flexural testing results show a steady increase in flexural strength up to 30% fibre content, beyond which the flexural strength decreases. These results suggest that the optimal fibre content and distribution for achieving the highest mechanical properties differ between different testing methods and potential applications.

The behaviour of short fibres in tensile test specimens differed noticeably from their response under bending load, as observed in the study. One reason for the different trends observed in tensile and flexural testing results could be the differences in the types of stresses applied in each testing method. Tensile testing applies a uniaxial tensile stress on the sample, while flexural testing applies interlaminar shear, tension on the outer bottom layers, and compression in the outer top layers. Specifically, the short fibres aligned themselves with the printing direction and the extruding direction of the filaments. The mechanical properties of the composite are significantly influenced by the orientation and dispersion of short fibres within it. In this study, it was observed that a composite with a lower fibre content (15%) demonstrated highest tensile strength, mainly because the fibres were more effectively aligned in the direction of the applied tensile force during the filament production and printing process, resulting in enhanced reinforcement. While a composite with a higher fibre content (30%) exhibited higher flexural strength due to the fibre orientation, which was more conducive to withstanding bending forces.

The authors have recently published a paper focused on the effect of adding different waste short carbon fibres (0 wt%, 2 wt%, 5 wt%, 8 wt%, 15 wt%, and 25 wt%) to recycled PP through 3D printing [37]. This research revealed that the 3D-printed specimens with 15 wt% carbon fibres exhibited the highest tensile and flexural strength, which differs from the findings of the current research on PP filaments reinforced with basalt fibres. In the

present study, the highest tensile strength was observed in specimens with 15 wt% basalt fibres, while the highest flexural strength was found in samples containing 30 wt% basalt fibres.

This discrepancy highlights the distinct mechanical properties imparted by different types of reinforcing fibres in PP composites. The carbon fibres, known for their high tensile modulus and strength, provided significant reinforcement at lower weight fractions, whereas the basalt fibres, with their excellent thermal stability and resistance to chemical attack, offered enhanced flexural properties at higher concentrations. These findings underscore the importance of selecting appropriate reinforcing materials and optimising their concentrations based on the desired mechanical performance of 3D-printed composites.

Further investigation into the microstructural differences and the interaction between the polymer matrix and the reinforcing fibres could provide deeper insights into the mechanisms driving these variations. Understanding these interactions is crucial for developing advanced composite materials tailored for specific applications, offering a balance between strength, flexibility, and durability.

5.5. Microscopy

The microscopic assessment of filaments and 3D printed samples provided valuable insights into the behaviour of PP reinforced with different compositions of short basalt fibres, as shown in Figure 7. The optical microscopy reveal dispersion of fibres throughout the PP matrix, indicating the absence of any agglomeration in the composite samples with low fibre weight fractions. Additionally, the cross-sectional images of the 3D printed samples in Figure 7 offer a glimpse into the interbead regions, revealing weak bonding and voids. As the fibre volume fraction increases, a transformation occurs in the interbead regions, transitioning from debonding or weak bonding (PP+5% BF) to the formation of voids (PP+50% BF). The alteration in viscosity and dynamics of thermoplastic flow due to the presence of fibres leads to challenges when attempting to fill the inter-bead regions, as depicted in Figure 7. These observations are consistent with the experimental results obtained from tensile testing of the printed specimens, as illustrated in Figure 4. The microscopic images of the fibre-reinforced filaments further confirm this trend, wherein an increase in the fibre volume fraction leads to the creation of voids within the manufactured filaments. The presence of these voids elucidates the underlying reason behind the observed reduction in the tensile strength of the short basalt fibre-reinforced filaments, as reported in Table 3. Overall, this comprehensive microscopic assessment sheds light on the structural characteristics of the developed filaments and printed components and provides valuable insights into their mechanical properties and performance.

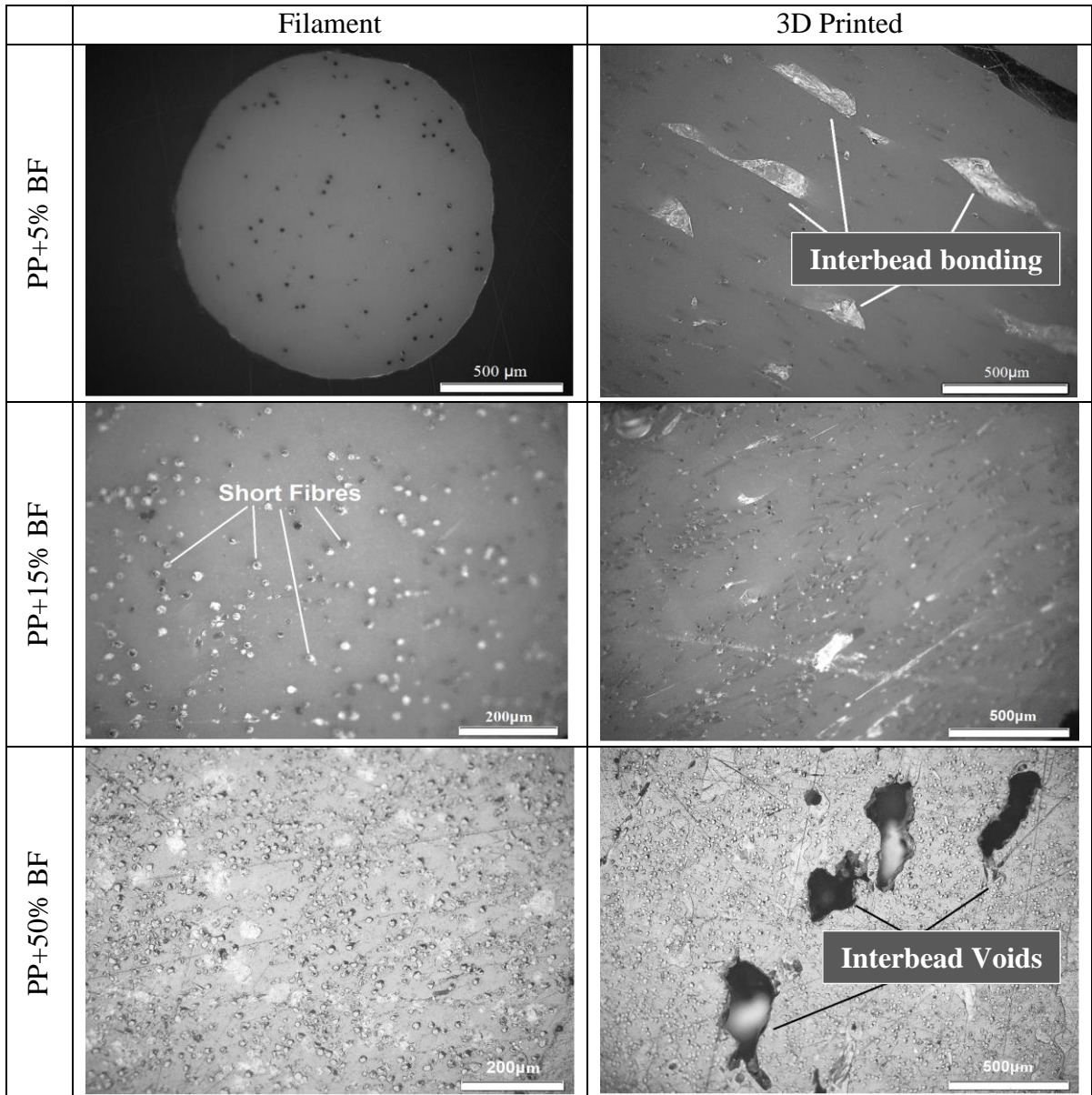


Figure 7: Optical microscopic images of fibre reinforced filaments and 3D printed samples.

SEM analysis was utilized to examine the fracture morphologies of filaments and MEX 3D printed tensile samples, with the aim of identifying the fracture modes. The fracture surface of MEX 3D printed tensile samples and fractured filaments, containing varying percentages of short basalt fibre (5%, 15%, 30%, and 50%), is depicted in Figure 8. Analysis of Figure 8 (A, C, E, and G) clearly indicates that, apart from the short fibre content, the dominant failure mode observed in the tested filaments is fibre pull-out. The smooth surface of the fibres dispersed within the matrix provides no evidence of fibre breakage in the fractured filaments.

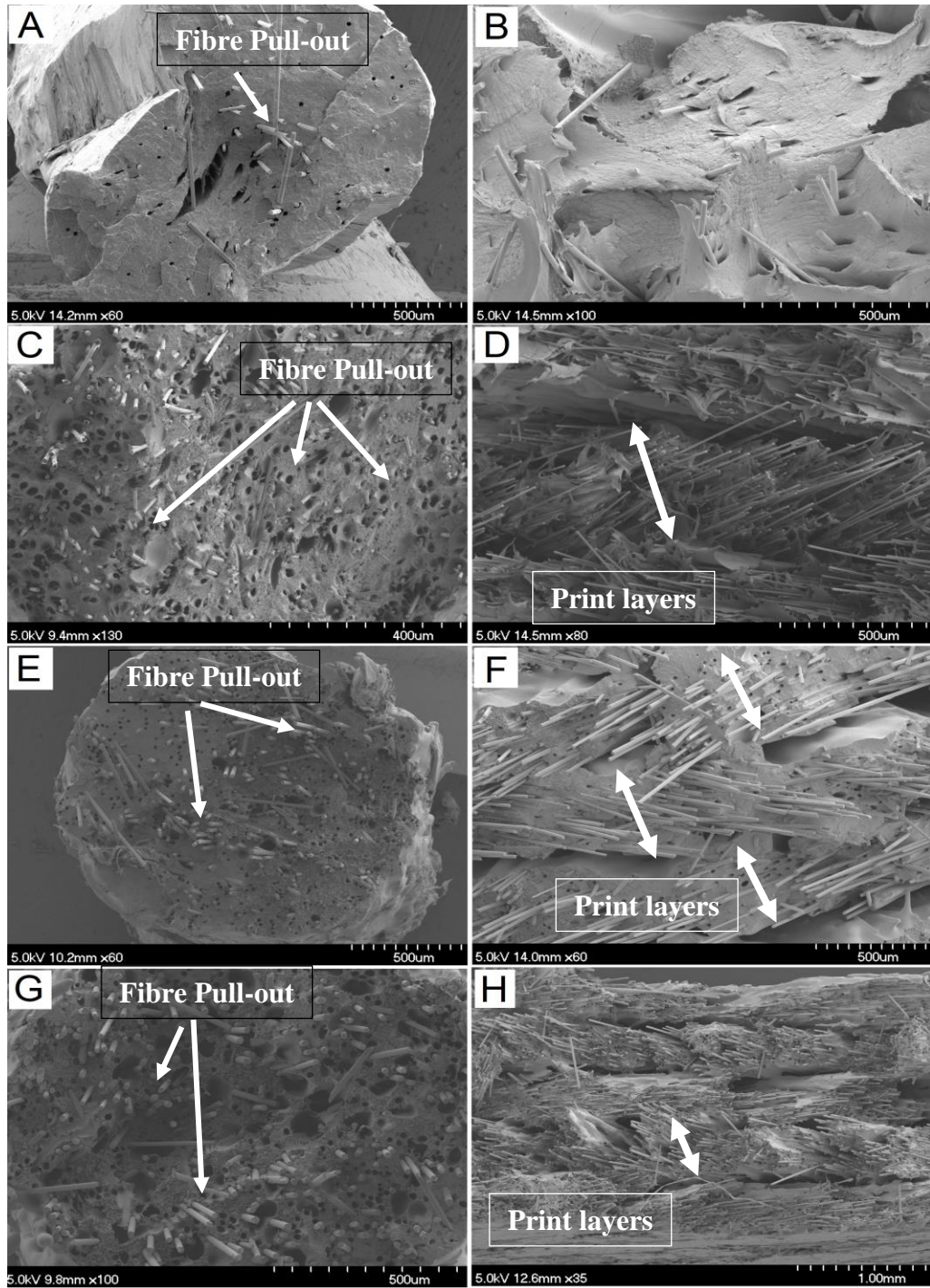


Figure 8: SEM images from the fractured surfaces of tensile tested fibre reinforced filaments and 3D printed samples, A) Filament with 5%BF, B) Printed sample with 5%BF, C) Filament with 15%BF, D) Printed sample with 15%BF, E) Filament with 30%BF, F) Printed sample with 30%BF, G) Filament with 50%BF, H) Printed sample with 50%BF.

The sample with a 5% weight fraction of short basalt fibre exhibits a more ductile fracture compared to the samples with higher fibre content. The SEM images in Figure 8 (C, E, and

G) also demonstrate the occurrence of voids in the manufactured filaments, which become more pronounced with an increase in fibre content. The fractured surfaces of the MEX 3D printed samples with 5%, 15%, 30%, and 50% short basalt fibre are displayed in Figure 8 (B, D, F, H), respectively. Based on Figure 8-B, it is evident that as the printing direction was ± 45 degrees relative to the tensile load direction, the short fibres exhibited their stiffening effect and shifted towards one side (specifically towards the left in Figure 8-B). The fracture surface exhibited characteristics of a ductile failure under tensile loading. Conversely, in Figure 8 (D, F, and H), clear instances of fibre pull-out and debonding between the printing layers were observed as the primary modes of failure in samples with high fibre volume fractions.

5.6. Differential Scanning Calorimetry

The DSC analysis revealed that the melting point of raw PP was $174.5 \pm 1.17^\circ\text{C}$, decreasing to $173.16 \pm 1.68^\circ\text{C}$ in PP filament and further to $170.5 \pm 1.15^\circ\text{C}$ in PP 3D printed samples. Similarly, the crystallization temperature decreased from $120.14 \pm 0.68^\circ\text{C}$ in raw PP to $118.81 \pm 1.91^\circ\text{C}$ in PP filament, and $117.7 \pm 0.22^\circ\text{C}$ in PP 3D printed samples. These results indicate a slight degradation during the filament extrusion process, causing a reduction in both melting and crystallization temperatures. This phenomenon aligns with prior research [38], attributing the decrease in thermal properties to the molecular weight reduction during filament making and 3D printing, resulting in enhanced molecular mobility and lower melting and crystallinity temperatures.

The percentage of crystallinity ($X_{c,DSC}$) was calculated using the following equation [39]:

$$X_{c,DSC} = \Delta H_f / \Delta H_{f0} \times 100 \% \quad (1)$$

ΔH_f represents the melting enthalpy measured in the heating experiments of the PP specimen, calculated from the peak area, while ΔH_{f0} denotes the theoretical value of enthalpy of fully crystalline PP, which was estimated at approximately 207 J/g [40]. The experimental analysis revealed variations in crystallinity percentages among different forms of polypropylene (PP). Specifically, raw PP exhibited the highest crystallinity at 37%, followed by PP filaments at 26.1%, and 3D printed PP materials at 24.2%. This indicates that the MEX process influences the crystallinity of PP materials compared to their raw form and filaments. These variations in crystallinity are affected by various factors related to the manufacturing processes. Processing conditions, such as temperature and cooling rates during filament extrusion and 3D printing, significantly impact the rate of crystallization and the final crystallinity of the PP material [37].

5. Conclusion

The findings of this study demonstrate that utilizing upcycled PP material combined with short basalt fibre proves to be a promising option for additive manufacturing technology. Through optimisation of essential parameters, this composite material exhibits favorable

characteristics (with a certain fibre weight fraction). Additionally, it holds the potential to address environmental concerns associated with waste plastic materials. The main findings of this research are summarized as follows:

- Various methods for achieving proper adhesion between the printed PP object and the print bed surface were explored. Rafts, brims, and glue did not provide satisfactory adhesion, while the use of 3-4 layers of polypropylene (PP) packing tape on the bed proved successful.
- Optimised parameters for printing PP reinforced with short basalt fibres were identified. Nozzle temperatures ranged from 245°C to 255°C depending on the weight fraction of basalt fibre. A bed temperature of 45°C was recommended for all compositions. Layer heights varied between 0.2mm and 0.45mm, with a thinner first layer for better adhesion and thicker subsequent layers to balance print quality and speed. Print speeds ranged from 8mm/s to 15mm/s, with slower speeds for higher fibre percentages. Flow rates were adjusted to maintain consistent print dimensions and structural integrity.
- The study revealed that the tensile strength of PP filaments increases with higher percentages of added basalt fibres up to 15% BF, and above that, the tensile strength decreases. Flexural testing of printed specimens demonstrates a continuous increase in flexural strength up to 30% fibre content, with a subsequent decrease.
- Cross-sectional images reveal weak bonding and the presence of voids in the interbead regions in the printed samples, with the type of defect transitioning from weak bonding to void formation as the fibre volume fraction increases. These observations align with the experimental results from tensile testing, where the presence of voids explains the reduction in tensile strength observed in the fibre-reinforced filaments.
- The extrusion process during filament production and 3D printing may cause degradation, leading to a slight reduction in both the melting and crystallization temperatures of PP.
- SEM analysis of filaments and MEX 3D printed tensile samples reveal the dominant failure mode to be fibre pull-out in the tested filaments and printed specimens, with no evidence of fibre breakage. The presence of voids in the manufactured filaments increases with higher fibre content. The extrusion process involved in filament making and 3D printing may induce degradation, leading to a slight decrease in the melting and crystallization temperatures of PP.

Declaration of Conflicting Interests

The author(s) declared no potential conflicts of interest with respect to the research, authorship, and/or publication of this article.

Funding

This project has received funding from the European Union's Horizon 2020 research and innovation programme under the Marie Skłodowska-Curie grant agreement No. 847402.

This publication has also emanated in part from research conducted with the financial support of Science Foundation Ireland under Grant number 16/RC/3872, 21/RC/10295_P2, and 22/IRDIFB/10946. For the purpose of Open Access, the author has applied a CC BY public copyright licence to any Author Accepted Manuscript version arising from this submission. This research was also supported by the Department of Business, Enterprise and Innovation and administered by Enterprise Ireland under the Disruptive Technologies Innovation Fund, MI-DRONE Project (Contract Ref: DT 2020 0221).

CRedit authorship contribution statement

Pouyan Ghabezi: Writing – original draft, Methodology, Investigation, Supervision, Funding acquisition. **Omid Sam-Daliri:** Writing – original draft, Methodology, Investigation, Funding acquisition. **Tomas Flanagan:** Writing – review & editing, Supervision, Resources, Funding acquisition. **Michael Walls:** Experimental methods, writing review & editing, Resources, Methodology. **Noel M. Harrison:** Writing – review & editing, Supervision, Concept development, Funding acquisition.

Data availability

Data will be made available on request.

References

- [1] Sauer M, Kuhnel M. Composites market report 2019. Carbon Composites. 2 (2019) 1-11.
- [2] Pegoretti A. Towards sustainable structural composites: A review on the recycling of continuous-fiber-reinforced thermoplastics. Advanced Industrial and Engineering Polymer Research. 4(2) (2021) 105-15.
- [3] ISO/ASTM 52900, Additive manufacturing: general: principles. Terminology. 640 (2015).
- [4] Shulga E, Karamov R, S. Sergeichev I, D. Konev S, I. Shurygina L, S. Akhatov I, et al. Fused filament fabricated polypropylene composite reinforced by aligned glass fibers. Materials. 13(16) (2020) 3442.
- [5] Sam-Daliri O, Ghabezi P, Steinbach J, Flanagan T, Finnegan W, Mitchell S, et al. Experimental study on mechanical properties of material extrusion additive manufactured parts from recycled glass fibre-reinforced polypropylene composite. Composites Science and Technology. 241 (2023) 110125.
- [6] Ghabezi P, Flanagan T, Walls M, Harrison NM. Degradation characteristics of 3D printed continuous fibre-reinforced PA6/chopped fibre composites in simulated saltwater. Progress in Additive Manufacturing. (2024) 1-14.
- [7] Ismail KI, Yap TC, Ahmed R. 3D-printed fiber-reinforced polymer composites by fused deposition modelling (FDM): fiber length and fiber implementation techniques. Polymers. 14(21) (2022) 4659.

- [8] Anwer A, Naguib HE. Multi-functional flexible carbon fiber composites with controlled fiber alignment using additive manufacturing. *Additive Manufacturing*. 22 (2018) 360-7.
- [9] Yang Z, Yang Z, Chen H, Yan W. 3D printing of short fiber reinforced composites via material extrusion: Fiber breakage. *Additive Manufacturing*. 58 (2022) 103067.
- [10] Somireddy M, Singh C, Czekanski A. Mechanical behaviour of 3D printed composite parts with short carbon fiber reinforcements. *Engineering Failure Analysis*. 107 (2020) 104232.
- [11] Sam-Daliri O, Ghabezi P, Flanagan T, Finnegan W, Mitchell S, Harrison N. Recovery of Particle Reinforced Composite 3D Printing Filament from Recycled Industrial Polypropylene and Glass Fibre Waste. *Proc World Congr Mech Chem Mater Eng*. 177 (2022) 3-4.
- [12] Kuo C-C, Chen J-Y, Chang Y-H. Optimization of process parameters for fabricating polylactic acid filaments using design of experiments approach. *Polymers*. 13(8) (2021) 1222.
- [13] Salleh FM, Hassan A, Yahya R, Azzahari AD. Effects of extrusion temperature on the rheological, dynamic mechanical and tensile properties of kenaf fiber/HDPE composites. *Composites Part B: Engineering*. 58 (2014) 259-66.
- [14] Yavas D, Zhang Z, Liu Q, Wu D. Interlaminar shear behavior of continuous and short carbon fiber reinforced polymer composites fabricated by additive manufacturing. *Composites Part B: Engineering*. 204 (2021) 108460.
- [15] Özden I, Scheithauer U, Iveković A, Kocjan A. Effect of infill strategy on the flexural strength of 3Y-TZP bars fabricated by thermoplastic 3D printing (T3DP). *Open Ceramics*. 14 (2023) 100367.
- [16] Agrawal AP, Kumar V, Kumar J, Paramasivam P, Dhanasekaran S, Prasad L. An investigation of combined effect of infill pattern, density, and layer thickness on mechanical properties of 3D printed ABS by fused filament fabrication. *Heliyon*. 9(6) (2023).
- [17] Benamira M, Benhassine N, Ayad A, Dekhane A. Investigation of printing parameters effects on mechanical and failure properties of 3D printed PLA. *Engineering Failure Analysis*. 148 (2023) 107218.
- [18] McNiffe E, Ritter T, Higgins T, Sam-Daliri O, Flanagan T, Walls M, et al. Advancements in functionally graded polyether ether ketone components: Design, manufacturing, and characterisation using a modified 3D printer. *Polymers*. 15(14) (2023) 2992.
- [19] Parker M, Inthavong A, Law E, Waddell S, Ezeokeke N, Matsuzaki R, et al. 3D printing of continuous carbon fiber reinforced polyphenylene sulfide: Exploring printability and importance of fiber volume fraction. *Additive Manufacturing*. 54 (2022) 102763.
- [20] Ngo TD, Kashani A, Imbalzano G, Nguyen KT, Hui D. Additive manufacturing (3D printing): A review of materials, methods, applications and challenges. *Composites Part B: Engineering*. 143 (2018) 172-96.
- [21] Almeshari B, Junaedi H, Baig M, Almajid A. Development of 3D printing short carbon fiber reinforced polypropylene composite filaments. *Journal of Materials Research and Technology*. 24 (2023) 16-26.

- [22] Ghabezi P, Flanagan T, Harrison N. Short basalt fibre reinforced recycled polypropylene filaments for 3D printing. *Materials Letters*. 326 (2022) 132942.
- [23] Cai R, Wen W, Wang K, Peng Y, Ahzi S, Chinesta F. Tailoring interfacial properties of 3D-printed continuous natural fiber reinforced polypropylene composites through parameter optimization using machine learning methods. *Materials Today Communications*. 32 (2022) 103985.
- [24] Alarifi IM. A performance evaluation study of 3d printed nylon/glass fiber and nylon/carbon fiber composite materials. *journal of materials research and technology*. 21 (2022) 884-92.
- [25] Vedrtnam A, Ghabezi P, Gunwant D, Jiang Y, Sam-Daliri O, Harrison N, et al. Mechanical performance of 3D-printed continuous fibre Onyx composites for drone applications: An experimental and numerical analysis. *Composites Part C: Open Access*. 12 (2023) 100418.
- [26] Yang D, Zhang H, Wu J, McCarthy ED. Fibre flow and void formation in 3D printing of short-fibre reinforced thermoplastic composites: An experimental benchmark exercise. *Additive Manufacturing*. 37 (2021) 101686.
- [27] Sang L, Han S, Li Z, Yang X, Hou W. Development of short basalt fiber reinforced polylactide composites and their feasible evaluation for 3D printing applications. *Composites Part B: Engineering*. 164 (2019) 629-39.
- [28] Vidakis N, Petousis M, Tzounis L, Maniadi A, Velidakis E, Mountakis N, et al. Sustainable additive manufacturing: mechanical response of polypropylene over multiple recycling processes. *Sustainability* 13 (1), 159. 2021.
- [29] Vidakis N, Petousis M, Maniadi A, Koudoumas E, Vairis A, Kechagias J. Sustainable additive manufacturing: Mechanical response of acrylonitrile-butadiene-styrene over multiple recycling processes. *Sustainability*. 12(9) (2020) 3568.
- [30] Vidakis N, Petousis M, Mountakis N, David CN, Sagris D, Das SC. Thermomechanical response of thermoplastic polyurethane used in MEX additive manufacturing over repetitive mechanical recycling courses. *Polymer Degradation and Stability*. 207 (2023) 110232.
- [31] Hanon MM, Zsidai L. Comprehending the role of process parameters and filament color on the structure and tribological performance of 3D printed PLA. *Journal of materials research and technology*. 15 (2021) 647-60.
- [32] Saini A, Elhattab K, Gummadi SK, Nadkarni GR, Sikder P. Fused filament fabrication-3D printing of poly-ether-ether-ketone (PEEK) spinal fusion cages. *Materials Letters*. 328 (2022) 133206.
- [33] Hadi A, Kadauw A, Zeidler H. The effect of printing temperature and moisture on tensile properties of 3D printed glass fiber reinforced nylon 6. *Materials Today: Proceedings*. 91 (2023) 48-55.
- [34] Tekinalp HL, Kunc V, Velez-Garcia GM, Duty CE, Love LJ, Naskar AK, et al. Highly oriented carbon fiber-polymer composites via additive manufacturing. *Composites Science and Technology*. 105 (2014) 144-50.
- [35] Elchalakani M, Yang B, Mao K, Pham T. 2 - Mechanical properties of fiber reinforced polymer (FRP) and steel bars. In: Elchalakani M, Yang B, Mao K, Pham T, editors. *Geopolymer Concrete Structures with Steel and FRP Reinforcements: Woodhead Publishing; 2023. p. 75-135.*

- [36] Li Z, Ma J, Ma H, Xu X. Properties and applications of basalt fiber and its composites. IOP Conference Series: Earth and Environmental Science: IOP Publishing; 2018. p. 012052.
- [37] Ghabezi P, Sam-Daliri O, Flanagan T, Walls M, Harrison NM. Circular economy innovation: A deep investigation on 3D printing of industrial waste polypropylene and carbon fibre composites. Resources, Conservation and Recycling. 206 (2024) 107667.
- [38] <https://www.tainstruments.com/pdf/literature/TA430.pdf>.
- [39] Petersmann S, Spoerk-Erdely P, Feuchter M, Wieme T, Arbeiter F, Spoerk M. Process-induced morphological features in material extrusion-based additive manufacturing of polypropylene. Additive Manufacturing. 35 (2020) 101384.
- [40] Yang C-G, Wang M-H, Zhang M-X, Li X-H, Wang H-L, Xing Z, et al. Supercritical CO₂ foaming of radiation cross-linked isotactic polypropylene in the presence of TAIC. Molecules. 21(12) (2016) 1660.